Journal of Applied Polymer Science

pH- and Temperature-Responsive IPN Hydrogels Based on Soy Protein and Poly(*N*-isopropylacrylamide-*co*-sodium acrylate)

Yong Liu,[1] Yingde Cui,[2] Miaochan Liao[3]

[1]School of Chemistry and Chemical Engineering, Zhaoqing University, Zhaoqing 526061, People's Republic of China
[2]Institute of Green Chemical Engineering, Zhongkai University of Agriculture and Engineering, Guangzhou 510225, People's Republic of China
[3]Department of Logistics Management, Zhaoqing University, Zhaoqing 526061, People's Republic of China
Correspondence to: Y. Liu (E-mail: lygdut@163.com) or Y. Cui (E-mail: cuizku@gmail.com)

ABSTRACT: pH- and temperature-responsive interpenetrating polymer network (IPN) hydrogels based on soy protein and poly(*N*-isopropylacrylamide-*co*-sodium acrylate) were successfully prepared. The structure and properties of the hydrogels were characterized by Fourier transform infrared spectroscopy, scanning electron microscopy, differential scanning calorimetry, and thermogravimetric analyzer. The equilibrium and dynamic swelling/deswelling behaviors and the drug release properties of the hydrogels responding to pH and/or temperature were also studied in detail. The hydrogels have the porous honeycomb structures, good miscibility and thermal stability, and good pH- and temperature-responsivity. The volume phase transition temperature of the hydrogels is ca. 40°C. Changing the soy protein or crosslinker content could be used to control the swelling behavior and water retention, and the hydrogels have the fastest deswelling rate in pH 1.2 buffer solutions at 45°C. Bovine serum albumin release from the hydrogels has the good pH and temperature dependence. The results show that the proposed IPN hydrogels may have potential applications in the field of biomedical materials such as in drug delivery systems. © 2013 Wiley Periodicals, Inc. J. Appl. Polym. Sci. **2014**, *131*, 39781.

KEYWORDS: stimuli-sensitive polymers; swelling; blends

Received 10 April 2013; accepted 20 July 2013
DOI: 10.1002/app.39781

INTRODUCTION

Soy protein is an abundant, renewable, and inexpensive natural protein, which is commonly used in food industry due to its nutritional value, functional properties, availability, and low cost. To date, some animal proteins, such as gelatin, collagen, casein, albumin, and whey protein, have been widely studied for delivering drugs, nutrients, bioactive peptides, and probiotic organisms.[1] Although soy protein-based materials have attracted more attention in adhesives,[2] nanofibers,[3] bioplastics,[4] films,[5] drug delivery,[6,7] tissue regeneration,[8] wound dressings,[9] etc., soy protein and its composites as new devices for biomedical utilization have not been fully investigated.

pH- and temperature-responsive hydrogels are extensively investigated in the biomedical field because these two factors are important inside the human body,[10] and also can be easily controlled and applied both in *in vitro* and *in vivo* conditions.[11] In the recent years, interests in a new class of hydrogels based on blends of natural and synthetic polymers are increasing,[12] especially in the blends with the stimuli-responsive polymers,[13] which is due to the blends having the advantages of the good biocompatibility and biodegradability from the natural polymers and the good mechanical properties and stimuli-responsivity from the synthetic polymers. To prepare these blends, an effective method is the interpenetrating polymer network (IPN) technology,[14,15] which can enhance their properties compared with conventional processing techniques.

Poly(*N*-isopropylacrylamide) (PNIPAAm) is a well-known temperature-responsive polymer with a volume phase transition temperature (VPTT) of ~32°C in aqueous solution,[16] whereas poly(acrylic acid) (PAA) is a typical pH-responsive polymer.[17] Both the polymers have been widely studied in biomedical field because of their responses to external stimuli.[18] Recently, increasing interests in designing the blends based on the natural polymers and PNIPAAm/PAA have been observed.[19,20] PNIPAAm/PAA has been used to blend with some natural polymers such as cellulose,[21,22] *k*-carrageenan,[23] chitosan,[24,25] xanthan,[26,27] alginate,[28] guar gum,[29,30] and gelatin[31] for the biomedical utilization, because these blends have good biocompatibility and biodegradability, and good stimuli-responsivity.

In this work, pH- and temperature-responsive IPN hydrogels based on soy protein and poly(*N*-isopropylacrylamide-*co*-sodium acrylate) were prepared. The hydrogels' properties, such as

Table I. Feed Compositions and Sample Codes of Hydrogels

Sample	SPI (g)	GA (mL)	NIPAAm (g)	AA (g)	BIS (g)	APS (g)	TEMED (μL)
IPN0	0.0	0.0	2.0	0.1	0.03	0.02	20
IPN1	0.4	0.2	2.0	0.1	0.03	0.02	20
IPN2	0.6	0.3	2.0	0.1	0.03	0.02	20
IPN3	0.4	0.2	2.0	0.1	0.04	0.02	20

network structures, miscibility, pH- and temperature-responsivity, were investigated. The swelling/deswelling kinetics and the drug release behaviors of the proposed hydrogels were also studied in detail.

EXPERIMENTAL

Materials

Soy protein isolate (SPI, Dupont Yunmeng Protein Company), *N*-isopropylacrylamide (NIPAAm, Tokyo Chemical Industry Company), acrylic acid (AA, Yongda Chemical Reagent Company), ammonium persulfate (APS, Yongda Chemical Reagent Company), *N*,*N*′-methylenebisacrylamide (BIS, Yongda Chemical Reagent Company), glutaraldehyde (GA, Kermel Chemical Reagent Company), and tetramethylethylenediamine (TEMED, Qianjin Chemical Reagent Company) were used as received. Bovine serum albumin (BSA, model drug) was purchased from Shanghai Sinopharm Chemical Reagent (Shanghai, China). Other reagents were analytical grade and used as received.

Preparation of Hydrogels

An amount of AA in a beaker was neutralized using 3.0*M* NaOH solutions and was adjusted to pH 11 by 0.1*M* NaOH solutions. The volume of the solutions was adjusted to 15 mL by adding deionized water. Then, NIPAAm and SPI were added into the solutions to dissolve and mix with continuously stirring. With nitrogen bubbling, GA, BIS, APS, and TEMED were added into the mixture. Finally, this mixture was injected immediately into PVC tubes (6 mm in diameter) to polymerize at 15°C in a low-temperature reactor for 24 h. The hydrogels obtained were cut into pieces of 3 mm in length and immersed in deionized water for 3 days to remove any unreacted residual reagents. The deionized water was refreshed every 4 h during this period. The swollen hydrogels were dried at room temperature and further dried to constant weight at 40°C in a vacuum oven. The feed compositions and sample codes are given in Table I.

FTIR Spectroscopy

Each dried sample ground with KBr was compressed into a tablet, and then was recorded the spectrum by a FTIR spectroscopy (Equinox 55, Bruker, Germany) with an average of 6 scans at a resolution of 0.2 cm^{-1}.

Glass Transition Temperature

The glass transition temperatures (T_g) of the dried samples were determined by a differential scanning calorimetry (DSC 204, Netzsch, Germany). First, all samples were heated from room temperature to 120°C at 20°C min^{-1} under a nitrogen atmosphere and then were cooled to room temperature. The samples were then reheated to 180°C at 10°C min^{-1}. T_g of the samples was determined from the second cycle. The midpoint of the inflection was taken as T_g.

Volume Phase Transition Temperature of Hydrogels

VPTT of the hydrogels was determined by DSC. First, the sample was swollen to equilibrium in deionized water at 25°C, and then about 10 mg of equilibrium swollen sample was placed into a hermetic aluminum pan and sealed tightly with a hermetic aluminum lid. The sample was heated from 20 to 55°C at 2°C min^{-1} under a nitrogen atmosphere. The onset point of the endothermic peak was taken as the VPTT.

Morphology

The samples swollen to equilibrium in deionized water were first frozen at −40°C for 10 h, and then freeze-dried for 24 h by a freeze dryer (LGJ-18, SHKY, China). The cross sections of the freeze-dried samples were sputter-coated with gold, and the morphology of the coated samples was examined using SEM (Quanta 400F, FEI, The Netherlands) with an acceleration voltage of 20 kV.

Thermogravimetry

The thermal stability of the samples was examined by a thermogravimetric analyzer (TG 209, Netzsch, Germany). All dried samples were heated from room temperature to 700°C under a nitrogen atmosphere at a heating rate of 10°C min^{-1}.

Swelling Ratio of Hydrogels

Pre-weighed dried hydrogels were immersed in deionized water (or in buffer solutions) to swell. At regular time intervals, the swelling hydrogels were taken out to weigh after the removal of the surface water through blotting with filter paper and then put back into the same vials. The swelling ratio was calculated by the following equation:

$$\text{Swelling ratio} = (M_t - M_d)/M_d$$

where M_d is the weight of dried hydrogels and M_t is the weight of swollen hydrogels at time t.

Deswelling Kinetics of Hydrogels

The swollen equilibrium hydrogels in deionized water at 25°C (or in pH 7.4 buffer solutions at 25°C) were weighed and then immersed in deionized water at 45°C (or in pH 1.2 buffer solutions at 25 or 45°C) to deswell. At regular time intervals, the hydrogels were taken out to weigh and then put back into the same vials. The water retention was defined as the deswelling ratio and was calculated by the following equation:

$$\text{Water retention} = (M_t - M_d)/(M_e - M_d)$$

where M_d is the weight of dried hydrogels, M_t is the weight of swollen hydrogels at the time t, and M_e is the weight of swollen hydrogels at the equilibrium state.

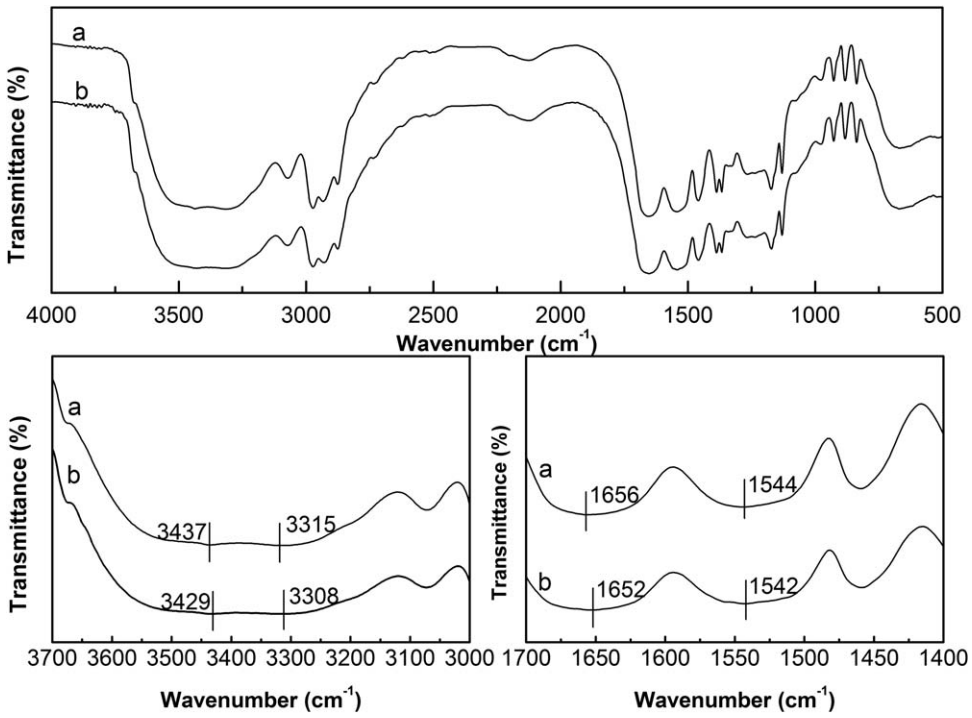

Figure 1. FTIR spectra of IPN0 (a) and IPN1 (b).

Drug Loading and Release of Hydrogels

BSA loading and release were according to the previous work.[1] Briefly, the blank hydrogels were immersed into the BSA aqueous solution (30 mg/mL) for 3 days at 4°C, and the BSA-loaded hydrogels were obtained by drying in a vacuum oven at 40°C to a constant weight. The BSA-loaded hydrogels were immersed in conical vials containing 30 mL of buffer solutions at various temperatures. The vials were closed and incubated in a thermostatic shaker (HY60, HCBioTch, China) with a speed of 60 rpm. At given time intervals, 3 mL of the solution was taken out to measure the amount of BSA release by a UV–vis spectrophotometer (760CRT, Lengguang, China) at 280 nm, and then put back into the same vial. The released concentration was obtained from the calibration curve. The cumulative release of BSA was calculated by the following equation:

$$\text{Cumulative release of BSA}\,(\%) = (W_t \times 100)/W$$

where W_t is the cumulative amount of BSA released at the time t and W is the initial amount of BSA loaded.

RESULTS AND DISCUSSION

Preparation of IPN Hydrogels

The natural polymers are usually biocompatible and biodegradable, whereas the synthetic polymers have good mechanical properties and thermal stability. According to the concept of biomimicry, bioartificial blends based on the natural polymers and the synthetic polymers have both the advantages of the natural and synthetic polymers for biomedical applications. In our previous work,[1] soy protein/PNIPAAm IPN hydrogels were investigated and their VPTTs were about 32°C. Human body temperature is around 37°C, especially when lesions occur in human body, such as influenza and tumors, the temperature is higher than 37°C,[32] and consequently, the hydrogels with the higher VPTT could expand their applications in the biomedical field. The IPN hydrogels based on soy protein and poly(*N*-isopropylacrylamide-*co*-sodium acrylate) were prepared using the simultaneous IPN method with GA crosslinking soy protein and BIS crosslinking NIPAAm and AA. Addition of AA in the feed not only can improve VPTT but endow pH responsivity of the hydrogels, while introduction of soy protein can endow the hydrogels with good biocompatibility and biodegradability.[33] Therefore, the proposed hydrogels have the advantages of biocompatibility, pH, and temperature responsivity for biomedical utilizations.

Structure and Morphology Analysis

The FTIR spectra of IPN0 and IPN1 are shown in Figure 1 and the data of their characteristic absorption bands are listed in Table II. In comparison with IPN0, no new characteristic absorption bands appear in IPN1, only some characteristic absorption bands shift to low wavenumber. The characteristic absorption band of ν_{N-H} shifts from 3315 (IPN0) to 3308 cm^{-1} (IPN1), whereas that of $\nu_{C=O}$ shifts from 1656 (IPN0) to 1652 cm^{-1} (IPN1). These characteristic absorption bands shifted to low wavenumber indicate that the presence of intermolecular hydrogen bonds among the polymeric molecular chains of soy protein, PNIPAAm, and sodium polyacrylate. Similar results were also reported by our previous research[1] and other researches.[34–37]

The morphological images of the cross sections of the freeze-dried hydrogels are shown in Figure 2. It is found that all the hydrogels show a porous honeycomb structure, which is created with the formed ice crystals serving as pore-forming agents

Table II. Characteristic Absorption Bands of Hydrogels

Hydrogels	Hydroxyl band (cm^{-1}) ν_{O-H}	ν_{N-H}	Amide I band (cm^{-1}) $\nu_{C=O}$	Amide II band (cm^{-1}) $\delta_{N-H} + \nu_{C-N}$
IPN0	3437	3315	1656	1544
IPN1	3329	3308	1652	1543

during the freezing step. The pore size of the hydrogels decreases in accordance with the increase of SPI content, while the thickness of the pore wall increases. The similar trend is also observed with the increase of BIS content. Therefore, varying SPI or BIS content can control different pore morphologies of the hydrogels, which can influence the diffusion of water and the swelling ratio of the hydrogels.

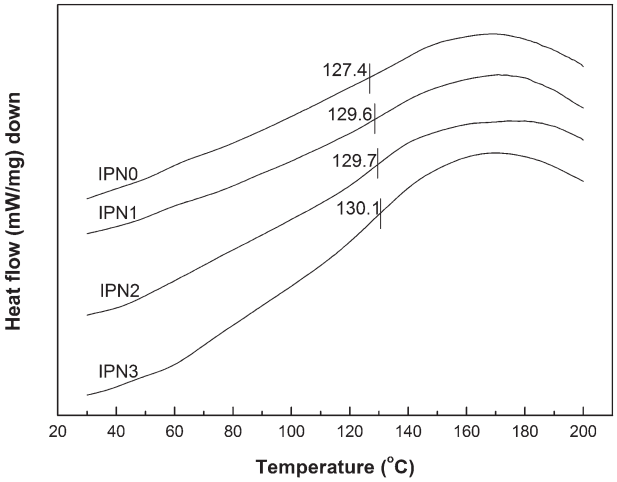

Figure 3. DSC thermograms of dried hydrogels.

Differential Scanning Calorimetry Analysis

The DSC thermograms of the hydrogels are shown in Figure 3. All the hydrogels have only one single T_g, which suggests that the proposed hydrogels have good miscibility. As seen from Figure 3, T_g gradually moves to higher temperature with increasing SPI or BIS content. It is reported that the value of T_g can be influenced by the formation of the hydrogen bonds in the hydrogels.[38,39] Therefore, the more SPI or BIS content, the stronger the hydrogen bonds in the blends, leading to the higher T_g. These results show that addition of SPI may improve the miscibility of the hydrogels.

DSC is a suitable method for detecting the VPTT of hydrogels according to the hydrophilic/hydrophobic phase transition. DSC thermograms of the swollen hydrogels are shown in Figure 4, in which the VPTTs of IPN0, IPN1, IPN2, and IPN3 are 38.9, 39.9, 40.1, and 40.5°C, respectively. The VPTT behavior is caused by the hydrophilic/hydrophobic balance in the hydrogel

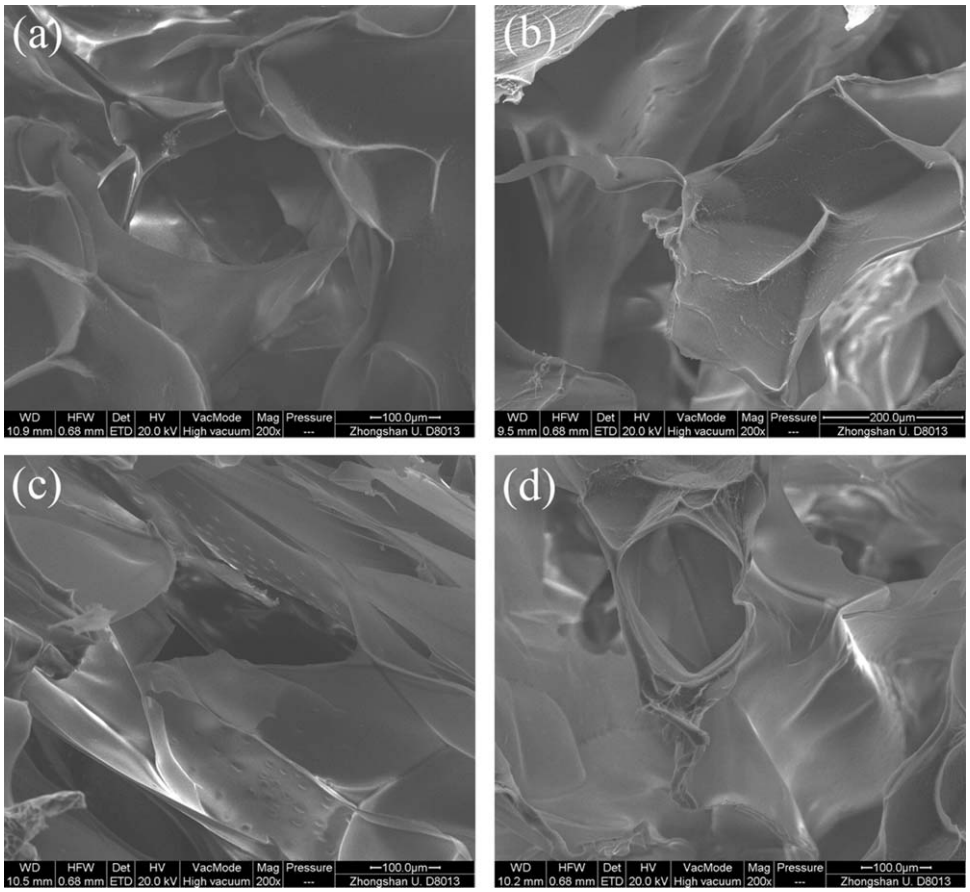

Figure 2. SEM micrographs of IPN0 (a), IPN1 (b), IPN2 (c), and IPN3 (d).

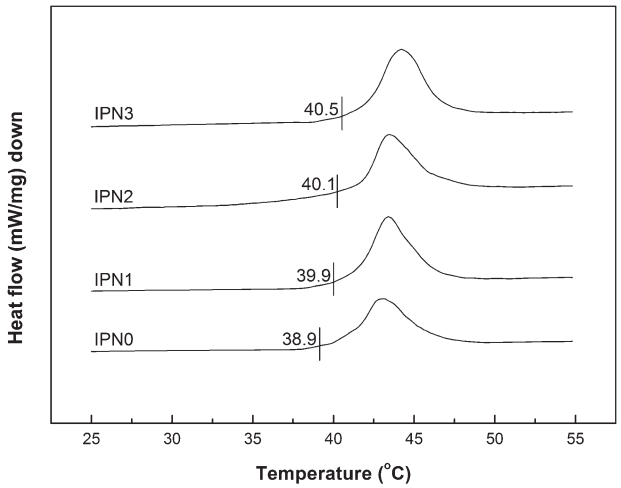

Figure 4. DSC thermograms of swollen hydrogels.

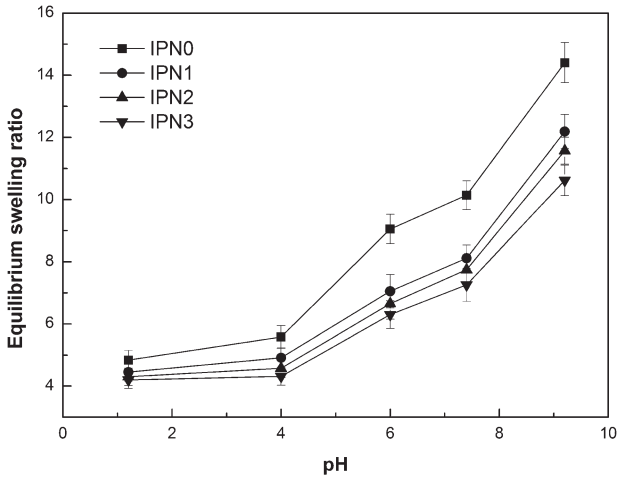

Figure 6. Equilibrium swelling ratios as a function of pH.

network, which can be affected by the hydrogen bonds,[1] resulting in different VPTT. The results also show that the VPTTs of the hydrogels are slightly influenced by the SPI and BIS content, and the VPTTs of the hydrogels are higher than that of PNIPAAm (about 32°C).

Thermogravimetric Analysis

The TGA thermograms of the hydrogels are depicted in Figure 5. As shown in Figure 5, all the samples have two weight loss stages. The first stage, the weight loss temperature is ca. 200°C and the weight loss ratio is ca. 5.43%, which is a consequence of acid anhydride formation and with the loss of water in the samples.[39,40] The second stage, the maximum weight loss temperature of IPN0, IPN1, IPN2, and IPN3 is 380.8, 390.4, 392.1, and 395.9°C, respectively, which is due to the polymer backbone decomposition. These results also show that increasing SPI or BIS content can increase the weight loss temperature due to the more hydrogen bonds produced by SPI and polymers and the more compact network structure caused by BIS.

pH and Temperature Responsivity

Equilibrium swelling ratio (ESR), namely, the swelling ratio of the hydrogels in a swelling equilibrium state, is used to evaluate the responsivity. The ESRs of the hydrogels in different buffer solutions ($I = 0.3M$) at 25°C and in deionized water at various temperatures are shown in Figures 6 and 7, respectively. As shown in Figure 6, all the samples have good pH responsivity. The ESRs are low in the pH range from 1.2 to 4.0, but high when pH > 4.0. Soy protein has high glutamic acid (11.9%) and aspartic acid (20.5%) contents and its isoelectric point is near pH 4.5,[17] and the pK_a of PAA is ca. 4.8. Consequently, when pH < 4.5, the carboxyl anion groups become carboxyl acid groups by protonating and thus form hydrogen bonds with the polar groups in the hydrogels, which results in the more compact network structure and the lower ESR. As pH > 4.8, the charge repulsive forces among the carboxyl anion groups are dominant, leading to the more expanding network structure and the higher ESR. The results in Figure 7 show that the hydrogels have good temperature responsivity and the VPTTs of the hydrogels are ca. 40°C. The hydrogels exhibit the high ESR as temperature below the VPTT, but low as temperature above the VPTT. This is attributed to the hydrophobic groups (—CH$(CH_3)_2$) and hydrophilic groups (—CONHR) in the hydrogels, which corresponds to the hydrophobic and hydrophilic regions, respectively. When temperature below the VPTT,

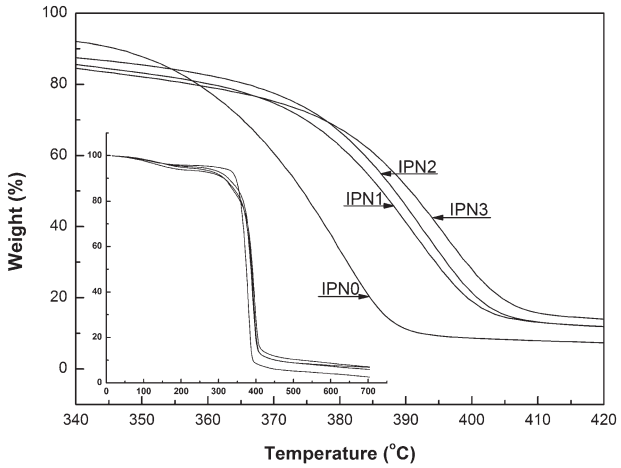

Figure 5. TGA thermograms of dried hydrogels.

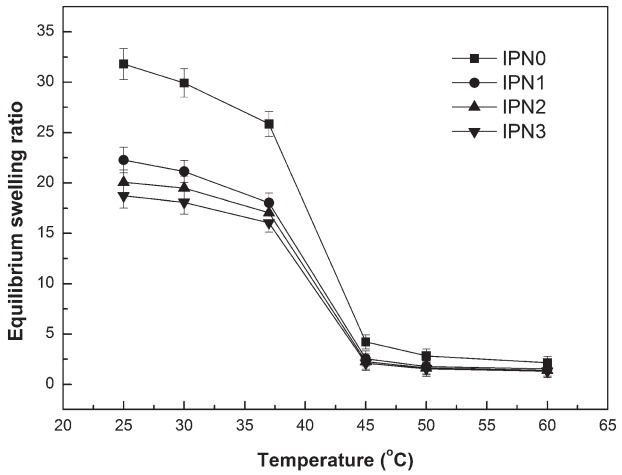

Figure 7. Equilibrium swelling ratios as a function of temperature.

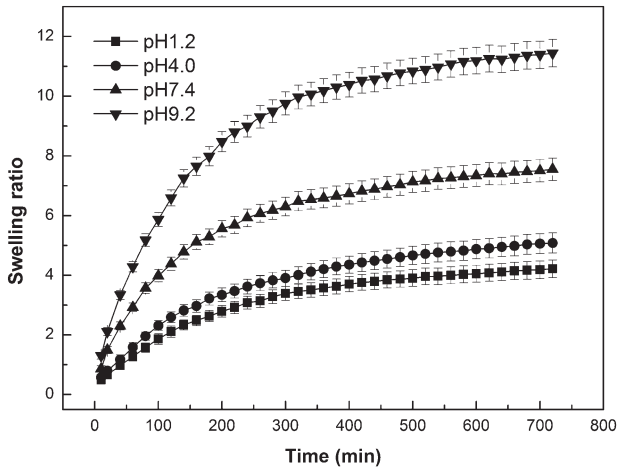

Figure 8. Swelling kinetics of hydrogels in different buffer solutions at 25°C.

the hydrogen bond interactions between the hydrophilic groups and water molecules are dominant, resulting in the higher ESR. Therefore, the interactions between the hydrophobic groups and water molecules are predominate with temperature above the VPTT, leading to the lower ESR. Additionally, both Figures 6 and 7 show that the ESR decrease with increasing SPI or BIS content. This is due to the more hydrogen bonds formed among the polymers with an increase of SPI and the more tight structure of the hydrogels with an increase of BIS, resulting in interactions between polymer and polymer predominating over the interactions between polymer and water, which leads to the lower ESR.

Swelling Kinetics

The swelling ratios of the hydrogels in different buffer solutions at 25°C and in deionized water at various temperatures are shown in Figures 8 and 9, respectively, and their images of the hydrogels at swelling equilibrium state are shown in Figure 10. As seen from Figure 8, the swelling ratio increases drastically from pH 1.2 to 9.2, and the swelling ratio is the lowest at pH 1.2, but the highest at pH 9.2. As the analyses above, the level of the swelling ratio depends on the degree of protonation of

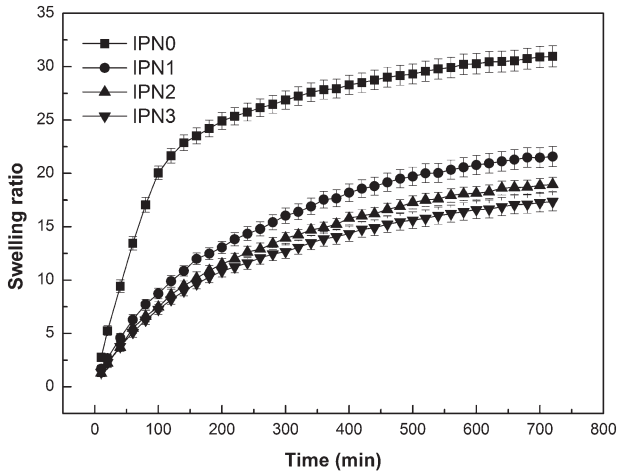

Figure 9. Swelling kinetics of hydrogels in deionized water at 25°C.

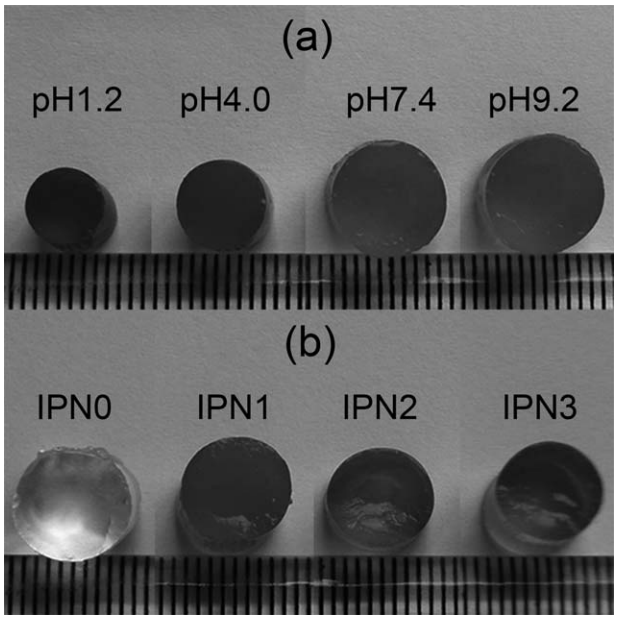

Figure 10. Images of hydrogels at swelling equilibrium state in buffer solutions (a) and deionized water (b).

the carboxyl anion groups, and Figure 10(a) further confirms this view. From Figure 9, the swelling ratio decreases with the increase of SPI or BIS content. It is due to, as mentioned above, the number of the formation of hydrogen bonds in the hydrogel and the degree of the tightness of hydrogel networks. It is also found that the swelling ratio of IPN0 is more than other tree hydrogels, which is caused by the more hydrogen bonds with SPI adding and the tighter network structure with BIS increasing. Figure 10(b) also confirms the results of Figure 9.

Deswelling Kinetics

The deswelling behaviors of IPN1 and IPN0 are shown in Figure 11. The water retention of IPN1 in pH 1.2 buffer solutions at 25°C (test 1), in deionized water at 45°C (test 3), and in pH 1.2 buffer solutions at 45°C (test 5) for a time of 720 min is 0.55, 0.66, and 0.31, respectively, whereas the water retention of IPN0 in pH 1.2 buffer solutions at 25°C (test 2), in deionized water at 45°C (test 4), and in pH 1.2 buffer solutions at 45°C (test 6) for a time of 720 min is 0.58, 0.68, and 0.35, respectively. The results show that the water retention of IPN1 is lower than that of IPN0, due to the soy protein reduces the density of the surface hydrophobic layer and enables water molecules to diffuse outward more easily. The water retention of test 5 and test 6 is much lower than that of tests 1, 2, 3, and 4. This is due to the coordination function of the protonation of carboxyl anion groups in pH 1.2 buffer solutions and the interactions between hydrophobic groups and water molecules at 45°C, causing the formation of more hydrogen bonds and the fast shrinkage of hydrogels. Therefore, the water retention is the lowest in pH 1.2 buffer solutions at 45°C.

To analyze the deswelling process quantitatively, a semi-logarithmic plot as a first-order rate analysis is used to the time dependence of the deswelling as: $\ln((M_t - M_d)/(M_e - M_d)) = -kt$, where k is the deswelling constant and t is time.[41,42] A greater k means a faster

deswelling process. From the value of k obtained by the plot of ln $((M_t - M_d)/(M_e - M_d))$ against t, the ratio of $k_{test\ 5}$ to $k_{test\ 3}$, $k_{test\ 5}$ to $k_{test\ 1}$, and $k_{test\ 1}$ to $k_{test\ 3}$ is 6.90, 5.14, and 1.34, respectively, and the ratio of $k_{test\ 6}$ to $k_{test\ 4}$, $k_{test\ 6}$ to $k_{test\ 2}$, and $k_{test\ 2}$ to $k_{test\ 4}$ is 6.35, 4.75, and 1.34, respectively. These results indicate that the deswelling rate of test 5 is 6.90 and 5.14 times faster than those of test 3 and test 1, respectively, and the deswelling rate of test 6 is 6.35 and 4.75 times faster than those of test 4 and test 2, respectively. Moreover, it is interesting that the ratio of $k_{test\ 5}$ to $k_{test\ 6}$, $k_{test\ 3}$ to $k_{test\ 4}$, and $k_{test\ 1}$ to $k_{test\ 2}$ is 1.20, 1.10, and 1.10, respectively. These results indicate that the hydrogels in pH 1.2 buffer solutions at 45°C have the fastest deswelling rate, and increasing the amount of soy protein can improve the deswelling rate, which indicates that the introduction of soy protein can improve the response rate of the hydrogels.

Drug Release from Hydrogels

The release curves of BSA at different conditions are shown in Figure 12. As seen in Figure 12, the BSA release rate from IPN1 in pH 7.4 buffer solutions at 37°C is faster than in pH 1.2 buffer solutions at 37°C, which indicates that the BSA release has a good pH dependence, whereas the BSA release rate from IPN1 in pH 7.4 buffer solutions at 37°C is lower than in pH 7.4 buffer solutions at 25°C, which indicates that the BSA release has a good temperature dependence. In pH 1.2 buffer solutions, the —COO— groups from soy protein and sodium acrylate in the hydrogels are protonated as —COOH groups, which results in the formation of hydrogen bonds and compact structure in the hydrogels, leading to the low release rate; but in pH 7.4 buffer solutions, the electrostatic repulsion between —COO— groups is dominant, which makes the hydrogels have expanding structure, causing fast release rate. At 25°C, the hydration structures form and make the polymer chain relaxation,[1] which results in the fast release rate; but at 37°C (near VPTT), the hydrophobic effect becomes dominant and causes the intertwining polymer chains and compact structure,[1] which leads to the low release rate. It is also found that the release rate of IPN1 is lower than that of IPN0 in the same condition. This is attributed to the intermolecular physical entanglements and the effect of hydrogen bonds increasing in the hydrogel network with adding soy protein to the feed, which results in the low release rate of IPN1. These results indicate that the hydrogels have good pH and temperature dependence, and modulating the content of soy protein can control the BSA release rate and release time.

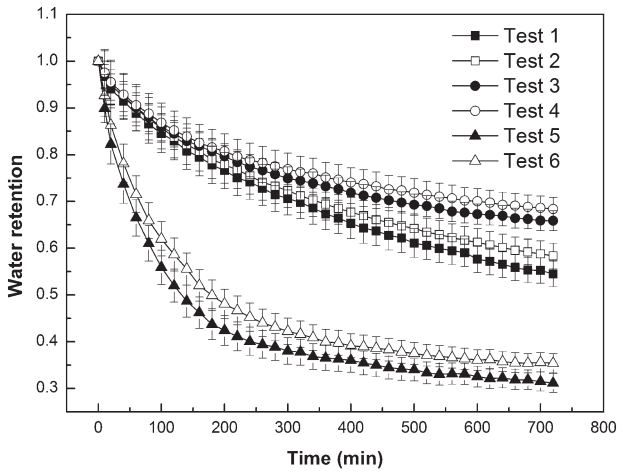

Figure 11. Water retention as a function of time in various conditions.

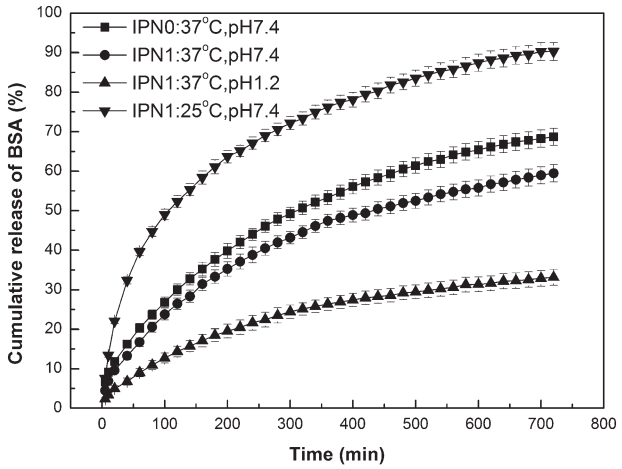

Figure 12. Dynamic release behaviors of BSA from hydrogels.

CONCLUSIONS

In summary, pH- and temperature-responsive IPN hydrogels composed of soy protein and poly(*N*-isopropylacrylamide-*co*-sodium acrylate) were successfully prepared in the presence of GA and BIS as the crosslinking agents and APS as the initiator. The VPTTs of the hydrogels are ca. 40°C, and the hydrogels have good pH- and temperature-responsivity, good miscibility, and thermal stability. Increasing the content of SPI can decrease the swelling rate but increase the deswelling rate. The BSA release from the hydrogels has good pH and temperature dependence. These hydrogels may be suitable for the controlled release of drugs.

ACKNOWLEDGMENTS

This work is financially supported by the Natural science Foundation of Guangdong Province (No. S2012040007710) and the Natural Science Foundation of Zhaoqing University (No. 201201).

REFERENCES

1. Liu, Y.; Cui, Y. *J. Appl. Polym. Sci.* **2011**, *120*, 3613.
2. Kumar, R.; Liu, D.; Zhang, L. *J. Biobased Mater. Bioenergy* **2008**, *2*, 1.
3. Vega-Lugo, A. C.; Lim, L. T. *J. Biobased Mater. Bioenergy* **2008**, *2*, 223.
4. Wang, N.; Zhang, L. *Polym. Int.* **2005**, *54*, 233.
5. Cho, S. Y.; Park, J. W.; Batt, H. P.; Thomas, R. L. *LWT-Food Sci. Technol.* **2007**, *40*, 418.
6. Chen, L.; Remondetto, G.; Rouabhia, M.; Subirade, M. *Biomaterials* **2008**, *29*, 3750.
7. Vaz, C. M.; van-Doeveren, P. F. N. M.; Reis, R. L.; Cunha, A. M. *Polymer* **2003**, *44*, 5983.

8. Chien, K. B.; Shah, R. N. *Acta Biomater.* **2012**, *8*, 694.
9. Peles, Z.; Zilberman, M. *Acta Biomater.* **2012**, *8*, 209.
10. Li, Z.; Shen, J.; Ma, H.; Lu, X.; Shi, M.; Li, N.; Ye, M. *Soft Matter* **2012**, *8*, 3139.
11. Ma, L.; Liu, M.; Liu, H.; Chen, J.; Gao, C.; Cui, D. *Polym. Adv. Technol.* **2010**, *21*, 348.
12. Sionkowska, A. *Prog. Polym. Sci.* **2011**, *36*, 1254.
13. Lee, K. Y.; Yuk, S. H. *Prog. Polym. Sci.* **2007**, *32*, 669.
14. Lipatov, Y. S. *Prog. Polym. Sci.* **2002**, *27*, 1721.
15. Gupta, N.; Srivastava, A. K. *Polym. Int.* **1994**, *35*, 109.
16. Tanaka, Y.; Kagami, Y.; Matsuda, A.; Osada, Y. *Macromolecules* **1995**, *28*, 2574.
17. Liu, Y.; Cui, Y. D.; Yin, G. Q.; Luo, L. Z. *J. Biobased Mater. Bioenergy* **2009**, *3*, 437.
18. Ma, J.; Fan, B.; Liang, B.; Xu, J. *J. Colloid Interface Sci.* **2010**, *341*, 88.
19. Jeong, B.; Kim, S. W.; Bae, Y. H. *Adv. Drug Delivery Rev.* **2012**, *64*, 154.
20. Klouda, L.; Mikos, A. G. *Eur. J. Pharm. Biopharm.* **2008**, *68*, 34.
21. Chang, C.; Han, K.; Zhang, L. *Polym. Adv. Technol.* **2011**, *22*, 1329.
22. Amin, M. C. I. M.; Ahmad, N.; Halib, N.; Ahmad, I. *Carbohydr. Polym.* **2012**, *88*, 465.
23. Mohanan, A.; Vishalakshi, B.; Ganesh, S. *Int. J. Polym. Mater.* **2011**, *60*, 787.
24. Chen, X.; Song, H.; Fang, T.; Bai, J.; Xiong, J.; Ying, H. *J. Appl. Polym. Sci.* **2010**, *116*, 1342.
25. Liu, J.; Wang, W.; Wang, A. *Polym. Adv. Technol.* **2011**, *22*, 627.
26. Hamcerencu, M.; Desbrieres, J.; Popa, M.; Riess, G. *Biomacromolecules* **2009**, *10*, 1911.
27. Bhattacharya, S. S.; Mishra, A.; Pal, D.; Ghosh, A. K.; Ghosh, A.; Banerjee, S.; Sen, K. K. *Polym.-Plast. Technol. Eng.* **2012**, *51*, 878.
28. Reddy, K. M.; Babu, V. R.; Rao, K. S. V. K.; Subha, M. C. S.; Rao, K. C.; Sairam, M.; Aminabhavi, T. M. *J. Appl. Polym. Sci.* **2008**, *107*, 2820.
29. Li, X. Y.; Wu, W. H.; Liu, W. Q. *Carbohydr. Polym.* **2008**, *71*, 394.
30. Li, X.; Wu, W.; Wang, J.; Duan, Y. *Carbohydr. Polym.* **2006**, *66*, 473.
31. Koul, V.; Mohamed, R.; Kuckling, D.; Adlerc, H. J. P.; Choudhary, V. *Colloids Surf. B* **2011**, *83*, 204.
32. Corry, P. M.; Armour, E. P. *Int. J. Hyperther.* **2005**, *21*, 769.
33. Song, F.; Tang, D. L.; Wang, X. L.; Wang, Y. Z. *Biomacromolecules* **2011**, *12*, 3369.
34. Chen, Y.; Zhang, L.; Gu, J.; Liu, J. *J. Membr. Sci.* **2004**, *241*, 393.
35. Silva, S. S.; Goodfellow, B. J.; Benesch, J.; Rocha, J.; Mano, J. F.; Reis, R. L. *Carbohydr. Polym.* **2007**, *70*, 25.
36. Wang, Q.; Du, Y.; Hu, X.; Yang, J.; Fan, L.; Feng, T. *J. Appl. Polym. Sci.* **2006**, *101*, 425.
37. Wu, W.; Li, W.; Wang, L. Q.; Tu, K.; Sun, W. *Polym. Int.* **2006**, *55*, 513.
38. Jin, S.; Liu, M.; Zhang, F.; Chen, S.; Niu, A. *Polymer* **2006**, *47*, 1526.
39. Adem, E.; Burillo, G.; Bucio, E.; Magaña, C.; Avalos-Borja, M. *Radiat. Phys. Chem.* **2009**, *78*, 549.
40. Garay, M. T.; Llamas, M. C.; Iglesias, E. *Polymer* **1997**, *38*, 5091.
41. Serizawa, T.; Wakita, K.; Akashi, M. *Macromolecules* **2002**, *35*, 10.
42. Zhang, J. T.; Keller, T. F.; Bhat, R.; Garipcan, B.; Jandt, K. D. *Acta Biomater.* **2010**, *6*, 3890.